Quantizing Chaos

Robert Gilmore
Physics Department, Drexel University, Philadelphia, Pennsylvania 19104, USA
(Dated: September 15, 2006, *Physical Review E*: To be submitted.)

We study strange attractors generated by two dimensional nonlinear oscillators. These attractors are embedded in a phase space that is a solid torus, $D^2 \times S^1$. Such strange attractors can be mapped in a locally 1-1 way to an entire set of strange attractors that are indexed by a pair of quantum numbers, n_1 and n_2. These integers are associated with the two generators of the homotopy group of the torus boundary, $\partial(D^2 \times S^1)$. The torsion and energy integrals for this two parameter family of locally identical strange attractors are simple functions of these two quantum numbers.

I. INTRODUCTION

It is common as well as convenient, and possibly misleading, to separate dynamical systems into two classes: autonomous and nonautonomous [1]. Familiar among the former are the Lorenz [2] and Rössler equations [3]. In three dimensions familiar examples of nonautonomous dynamical systems are periodically driven two dimensional nonlinear oscillators. In three dimensions the phase spaces for autonomous and nonautonomous dynamical systems are R^3 and $D^2 \times S^1$, where D^2 is a disk (bounded region in R^2) on which coordinates (X, Y) are defined and S^1 is a circle with $\theta/2\pi \leftrightarrow t/T_d$ relating the topology of the torus with the dynamics. Here T_d is the period of the harmonic driving term.

The forcing terms of a periodically driven nonlinear oscillator exhibit a periodic symmetry under $(X, Y, t) \to (X, Y, t + T_d)$. Under rather general terms they also exhibit an internal order-two symmetry under $(X, Y, t) \to (-X, -Y, t + \frac{1}{2}T_d)$. This two-fold internal symmetry can be removed by projecting the motion (periodic or chaotic) onto "the" van der Pol plane [1, 4, 5]. This is a rotating plane whose rotation angular frequency, Ω, is synchronized with the angular frequency of the forcing term, $\omega_d = 2\pi/T_d$. In fact, there are two counterrotating van der Pol planes that create a $2 \to 1$ map of a strange attractor of period T_d to an "image" attractor with no internal symmetry and half the period: $T_{image} = \frac{1}{2}T_d$.

There is a growing understanding of dynamical systems and their strange attractors with some symmetry and locally identical (diffeomorphic) dynamical systems with less symmetry, the same symmetry but different topology, different symmetry, or more symmetry [6–8]. Most of these studies have been carried out for autonomous dynamical systems. In the present work we carry out such studies for nonautonomous dynamical systems such as periodically driven two dimensional nonlinear oscillators [4, 5, 9].

We find for each periodic strange attractor in $D^2 \times S^1$ that there is an entire set of locally diffeomorphic strange attractors. These are distinguished by two integer quantum numbers, n_1 and n_2, with $n_1 \geq 1$ and n_2 relatively prime to n_1. Two such attractors, labeled (n_1, n_2) and $(n_1, n_2)'$, are distinct if $(n_1, n_2) \neq (n_1, n_2)'$; they are globally diffeomorphic if $n_1 = n_1'$ and distinct if $n_1 \neq n_1'$ or $n_2 \neq n_2'$. The two quantum numbers are related to the two generators of the homotopy group of the boundary of a torus, $\partial(D^2 \times S^1)$, containing a certain "universal image" attractor [4]. The quantum number n_1 is related to the longitude; dynamically, it describes the order of the cover [6–8]. The quantum number n_2 is identified with the meridian; dynamically, it describes the torsion of the attractor [10].

We introduce two integrals to characterize the entire family of attractors. One is an averaged torsion integral, the second is an averaged energy integral. These integrals depend smoothly on the quantum numbers (n_1, n_2). The values of these integrals can be plotted on universal curves that can be computed from the parameters of any single member of this family. The "universal image attractor" is typically chosen as the member of this family with least symmetry that minimizes the energy integral. These ideas are illustrated using a strange attractor generated by a version of the periodically driven van der Pol oscillator [1, 4, 5].

The structure of this paper is as follows. In Sect. II we introduce a large class of two dimensional nonlinear oscillators with periodic drive. The two-fold internal symmetry under $(X, Y, t) \to (-X, -Y, t + \frac{1}{2}T_d)$ is exhibited. In Sect. III we introduce $2 \to 1$ and $1 \to 1$ mappings of the strange attractor onto phase spaces $D^2 \times S^1$ using coordinate systems rotating harmonically with $\Omega = k\omega_d$, k integer. For k even the mappings are $1 \to 1$ global diffeomorphisms, for k odd they are $2 \to 1$ local diffeomorphisms. As $|k|$ increases the mapped attractor becomes more tightly wound up.

Torsion and energy integrals are introduced in Sect. IV, where they are computed analytically and numerically. In Sect. V we introduce the idea of a "universal image attractor." In Sect. VI we map the universal image in a locally 1-1 way onto n_1-fold covering strange attractors with $\Omega = (n_2/n_1)\omega_1$, where ω_1 is the angular frequency of the universal image attractor: $\omega_1 = 2\pi/(\frac{1}{2}T_d) = 2\omega_d$. The torsion and energy integrals are presented for a large number of strange attractors (n_1, n_2) in this class. In Sect. VII we make a number of remarks about the class of strange attractors constructed and the relation of the methods used for this construction with traditional ideas in physics and mathematics. In Sect. VIII we summarize these results.

II. DRIVEN NONLINEAR OSCILLATORS

Two-dimensional nonlinear oscillators $\dot{\mathbf{X}}_i = \mathbf{F}_i(\mathbf{X})$:

$$\frac{d}{dt}\begin{bmatrix} X \\ Y \end{bmatrix} = \begin{bmatrix} F_1(X,Y) \\ F_2(X,Y) \end{bmatrix} \tag{1a}$$

have been used to model many physical systems. Such dynamical systems cannot exhibit chaotic behavior since they are two dimensional. If they are periodically driven they can behave chaotically and generate strange attractors. The driven systems have the form $\dot{\mathbf{X}}_i = \mathbf{F}_i(\mathbf{X}) + \mathbf{t}$:

$$\frac{d}{dt}\begin{bmatrix} X \\ Y \end{bmatrix} = \begin{bmatrix} F_1(X,Y) \\ F_2(X,Y) \end{bmatrix} + \begin{bmatrix} a_1 \sin(\omega_d t + \phi_1) \\ a_2 \sin(\omega_d t + \phi_2) \end{bmatrix} \tag{1b}$$

In most instances a_1 or a_2 is taken to be zero and ϕ_i is chosen as 0 or $\pi/2$, for convenience. The relevant phase space for such periodically driven nonlinear oscillators is the solid torus $D^2 \times S^1$, where the geometric coordinate, θ, which parameterizes the S^1 part of the solid torus, is related to the dynamical parameter, t, the physical time, by

$$\frac{\theta}{2\pi} \leftrightarrow \frac{t}{T_d} \tag{2}$$

In many instances the forcing functions $F_i(X,Y)$ are taken to be odd: $F_i(-X,-Y) = -F_i(X,Y)$, for physical reasons. In such cases the dynamical systems equations (1b) are unchanged ("equivariant") under the transformation $(X,Y,t) \to (-X,-Y,t+\frac{1}{2}T_d)$. If a strange attractor of period T_d is generated by this dynamics, it shares the same internal two-fold symmetry.

The two-fold internal symmetry can be removed by projecting the phase space coordinates (X,Y) to a harmonically rotating set of axes [1, 4, 5], so that the coordinates in the rotating coordinate system are

$$\begin{bmatrix} u(t) \\ v(t) \end{bmatrix} = \begin{bmatrix} \cos\Omega t & -\sin\Omega t \\ \sin\Omega t & \cos\Omega t \end{bmatrix} \begin{bmatrix} X(t) \\ Y(t) \end{bmatrix} \tag{3}$$

with $\Omega = \pm\omega_d$. Under this transformation $(u,v,t) \to (+u,+v,t+\frac{1}{2}T_d)$. The coordinate transformation (3) removes the internal symmetry and reduces the periodicity of the image attractor(s) to $T_1 = \frac{1}{2}T_d$. The image attractor has period one in a torus $D^2 \times S^1$ with the following identification between the geometric coordinate θ of the torus and the dynamical coordinate t of the attractor:

$$\frac{\theta}{2\pi} \leftrightarrow \frac{t}{\frac{1}{2}T_d} \tag{4}$$

The two choices $\Omega = \pm\omega_d$ define two counter-rotating van der Pol planes.

The dynamical system equations in the rotating coordinate system are

$$\frac{d}{dt}\begin{bmatrix} u \\ v \end{bmatrix} = R\mathbf{F}(R^{-1}\mathbf{u}) + R\mathbf{t} + \Omega \begin{bmatrix} -v \\ +u \end{bmatrix} \tag{5}$$

The first term on the right is the original forcing term in Equ. (1b), without the periodic drive. This is seen in a rotating coordinate system. The matrix $R = R(\Omega t)$ is the rotation matrix in Equ. (3), and $R^{-1}(\Omega t) = R(-\Omega t)$ is its inverse. The second term in this equation is the periodic drive at angular frequency ω_d, seen in the rotating coordinate system. As this term contains products of sines and cosines at the driving and rotating frequencies ω_d and Ω, it can be expressed as in terms of sines and cosines of sum and difference frequencies $|\Omega \pm \omega_d|$. The last term in this equation is the Coriolis term.

The ideas presented below will be illustrated by application to the following version of the van der Pol equations:

$$\begin{aligned} \dot{X} &= bY + (c - dX^2)X \\ \dot{Y} &= -X + A\sin(\omega_d t) \end{aligned} \tag{6}$$

with the following values of the control parameters: $(A,b,c,d,\omega_d) = (0.25, 0.7, 1.0, 10.0, \pi/2)$.

III. HARMONIC ROTATIONS: IMAGES

Harmonic rotations are synchronized with the drive: $\Omega = k\omega_d$, k integer. They induce the following symmetry:

$$(u,v,t) \to (-(-1)^k u, -(-1)^k v, t + \frac{1}{2}T_d) \tag{7}$$

For k even these rotations induce a global 1-1 diffeomorphism between the original strange attractor with two-fold internal symmetry and period T_d and the resulting mapped attractor, with identical internal symmetry and period. For k odd all the resulting image attractors have period $\frac{1}{2}T_d$ and no residual internal symmetry. They are all $2 \to 1$ locally diffeomorphic images of the original strange attractor ($k = 0$) and its diffeomorphic siblings (k even). Attractors constructed with k odd are all globally diffeomorphic with each other but topologically inequivalent.

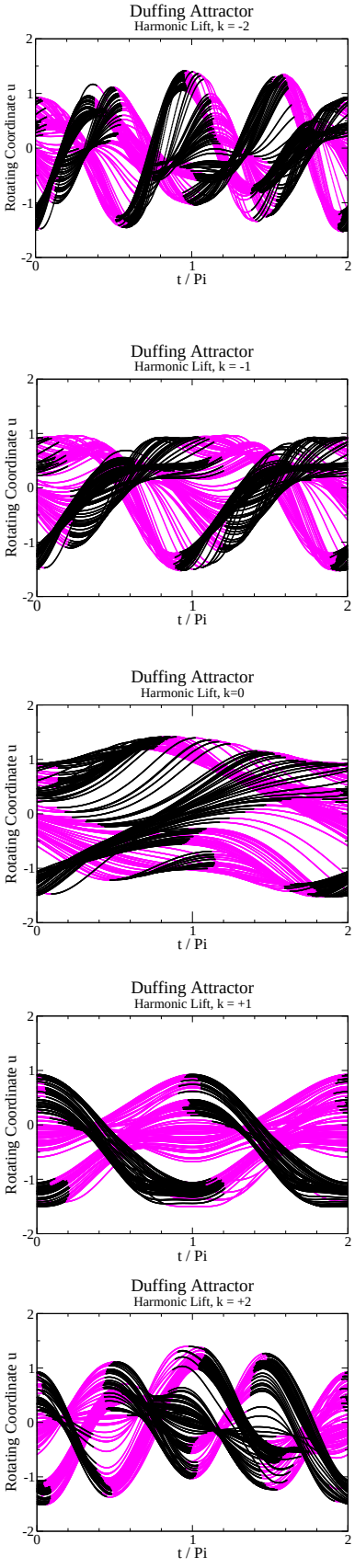

FIG. 1: Strange attractors in the torus $D^2 \times S^1$ projected from the van der Pol strange attractor, with parameter values $(a, b, c, d, \omega) = (0.25, 0.7, 1.0, 10.0, \pi/2)$ and rotation index k, $-2 \le k \le +2$.

The integer k serves to increase the torsion of the attractor. This can be seen in Figure 1. This consists of a series of plots of $u(t)$ vs. t for $0 \le t \le T_d$ for the van der Pol attractor Equ. (6). In this series of figures the integer k ranges from -2 to $+2$. The orbit segments with $v > 0$ are plotted darker than segments with $v < 0$. This figure illustrates three features of projections using rotating planes: (a) the rotation of the image attractor changes direction as k increases through 0; (b) the attractors become more tightly wound as $|k|$ increases. (c) the periodicity of the strange attractor alternates between T_d (k even) and $\frac{1}{2}T_d$ (k odd).

IV. TORSION AND ENERGY INTEGRALS

Two integrals express the relation between the rotation of the plane and the apparent rotation of the strange attractor as seen from that plane. These are the (averaged) torsion and energy integrals:

$$L = L(0) = \lim_{\tau\to\infty} \frac{1}{\tau} \int_0^\tau X dY - Y dX \tag{8}$$

$$K = K(0) = \lim_{\tau\to\infty} \frac{1}{\tau} \int_0^\tau \frac{1}{2}(\dot{X}^2 + \dot{Y}^2) dt \tag{9}$$

The integrals $L(\Omega)$ and $K(\Omega)$ for a strange attractor with coordinates (u, v) in a coordinate system rotating with angular velocity Ω are related to the integrals $L(0)$ and $K(0)$ of the original attractor with coordinates (X, Y) (and $\Omega = 0$) by

$$\begin{aligned} L(\Omega) &= \langle u\dot{v} - v\dot{u} \rangle \\ &= \langle X\dot{Y} - Y\dot{X} \rangle + \Omega\langle (X^2 + Y^2) \rangle \\ &= L(0) + \Omega\langle R^2 \rangle \end{aligned} \tag{10}$$

$$\begin{aligned} K(\Omega) &= \langle \frac{1}{2}(\dot{u}^2 + \dot{v}^2) \rangle \\ &= \langle \frac{1}{2}(\dot{X}^2 + \dot{Y}^2) \rangle + \Omega\langle (X\dot{Y} - Y\dot{X}) \rangle \\ &\quad + \frac{1}{2}\Omega^2\langle (X^2 + Y^2) \rangle \\ &= K(0) + \Omega L(0) + \frac{1}{2}\Omega^2\langle R^2 \rangle \end{aligned} \tag{11}$$

If the mean moment of inertia $\langle R^2 \rangle = \lim_{\tau\to\infty} \frac{1}{\tau} \int_0^\tau (u^2 + v^2) dt$, which is independent of Ω, and the torsion $L(0)$ and kinetic energy $K(0)$ are known for the original strange attractor, they can be computed for any projections of that attractor into harmonically rotating planes.

In Fig. 2 we plot the average torsion integral for strange attractors projected from the van der Pol strange attractor, for values of k ranging from -10 to $+10$. Since $\Omega = k\omega_d$ we have plotted $L(k)/(\omega_d\langle R^2 \rangle)$, so that the steps between successive values of the integers k should be integer: $(L(k+1) - L(k))/(\omega_d\langle R^2 \rangle) = +1$. This result is evident in Fig. 2. In Fig. 3 we plot $K(\Omega)$ vs. k in the same range of values. These graphs show clearly that the

torsion increases linearly with k and the kinetic energy depends quadratically on k. In fact, the averaged energy integral is a quadratic function of the averaged torsion integral:

$$K(\Omega) - K(0) = \frac{L(\Omega)^2}{2\langle R^2\rangle} - \frac{L(0)^2}{2\langle R^2\rangle} \tag{12}$$

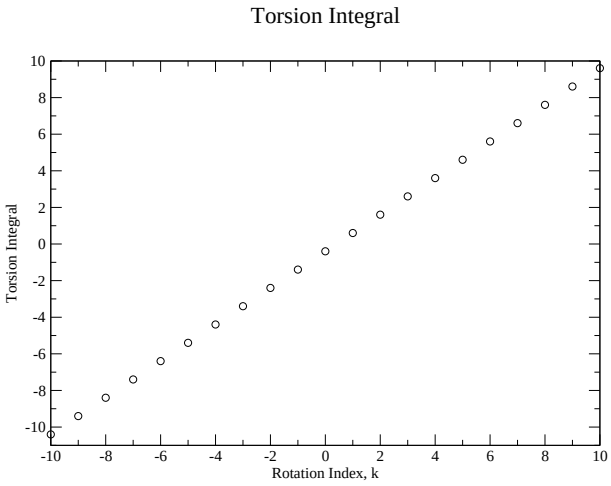

FIG. 2: Torsion Integral. The display is of the long term limit defined in Equ. (10) divided by $\omega_d\langle u^2 + v^2\rangle$, so that the integral changes by $\Delta L = +1$ when $\Delta k = +1$. The zero crossing occurs at "k" $= 0.398$.

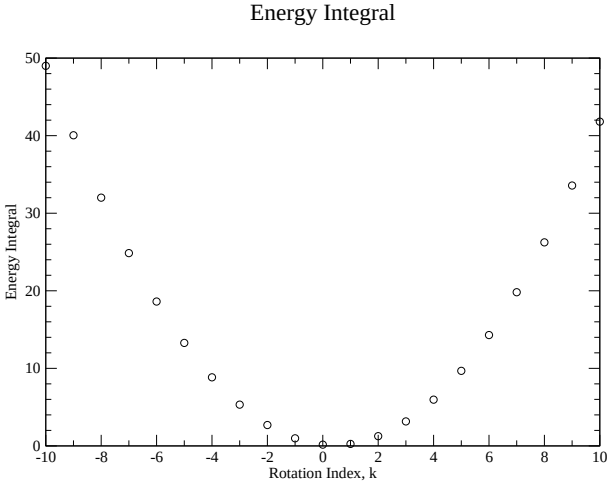

FIG. 3: Energy Integral. The value depends quadratically on k, with a minimum between $k = 0$ and $k = 1$ at the zero crossing of the Torsion Integral.

V. UNIVERSAL IMAGE

The energy plot strongly suggests that one of the rotating van der Pol planes ($k = +1$) is preferred over the other ($k = -1$). In this preferred rotating plane the rotational energy is lower, as is the absolute value of the torsion integral. This can also be seen by comparing Fig. 1(b) with Fig. 1(d). We identify the image attractor in this coordinate system as "the" universal image attractor for the control parameters shown. All attractors created below will be lifts ($n_1 > 1$) or images ($n_1 = 1$) of this preferred (with least symmetry and energy) universal image attractor.

VI. SUBHARMONIC ROTATIONS: COVERS

Once a universal image attractor has been identified, a series of rotational transformations can be carried out on that attractor. This procedure is almost exactly the same as that described in Sect. II. The relation between the torsion and energy integrals given in Sect. IV remains unchanged, with the understanding that $L(0)$ and $K(0)$ are measured for the universal image attractor of period $T_1 = \frac{1}{2}T_d$ and angular frequency $\omega_1 = 2\omega_d$.

The only difference is a notable one. The rotation frequency can be subharmonically related to the angular frequency ω_1 of the periodically driven image attractor: $\Omega = (p/q)\omega_1 = (n_2/n_1)\omega_1$. Strange attractors generated by these rotations are periodic with period $T_{(n_1,n_2)} = n_1 T_1$. For these attractors the relation between the geometric parameter θ describing position in the torus $D^2 \times S^1$ and the dynamical parameter t is

$$\frac{\theta}{2\pi} \leftrightarrow \frac{t}{T_{(n_1,n_2)}} = \frac{t}{n_1 T_1} \tag{13}$$

The transformation with $p = 0, q = 1$ or $(n_1, n_2) = (1, 0)$ reproduces the universal image. The transformation with $(n_1, n_2) = (2, -1)$ or $p/q = -1/2$ generates a double cover ($n_1 = 2$) that is identical to the original van der Pol attractor, for the covering coordinates are related to the image coordinates by

$$R(\frac{-1}{2}\omega_1 t)R(+1\omega_d t) = R(-\frac{1}{2}2\omega_d t)R(+1\omega_d t) = I_2 \tag{14}$$

The double covers of the image attractor with $(n_1, n_2) = (2, -1)$ and $(2, +1)$ are shown in Fig. 4. The attractor with $p/q = -1/2$ is clearly related to the original van der Pol attractor (Fig. 1 (c)). The two are related by a rigid rotation.

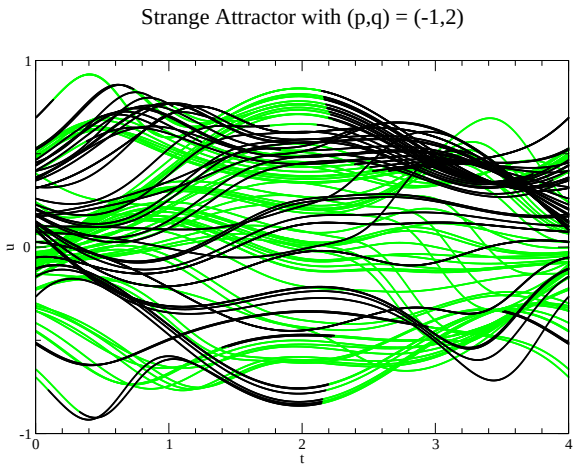

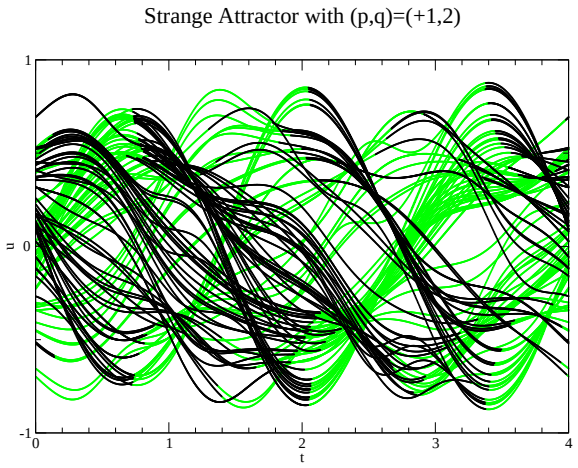

FIG. 4: Projections of the strange attractors with quantum numbers $p/q = n_2/n_1$ with $(n_1, n_2) = (2, -1)$ and $(2, +1)$ onto the (u, t) plane.

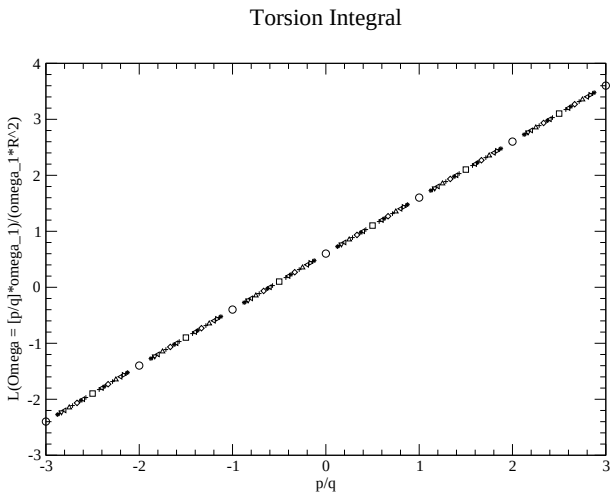

FIG. 5: Torsion Integral for everywhere locally diffeomorphic but topologically inequivalent strange attractors with quantum numbers (n_1, n_2), with $1 \leq n_1 \leq 8$ and $-3 \leq n_2/n_1 \leq +3$.

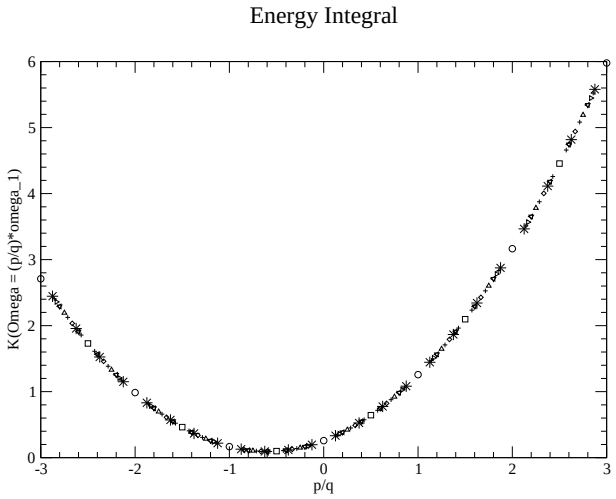

FIG. 6: Energy Integral for everywhere locally diffeomorphic but topologically inequivalent strange attractors with quantum numbers (n_1, n_2), with $1 \leq n_1 \leq 8$ and $-3 \leq n_2/n_1 \leq +3$.

The torsion and energy integrals behave linearly and quadratically with $\Omega = (n_2/n_1)\omega_1$. The values of the torsion and energy integrals for all attractors of type (n_1, n_2), with $1 \leq n_1 \leq 8$ and $-3 \leq n_2/n_1 \leq +3$, with n_1 and n_2 relatively prime, have been estimated numerically with $\tau = 1000T_d$. The results are shown in Fig. 5 and Fig. 6. The torsion has been scaled by $\omega_1\langle R^2\rangle$ so that $L(\omega_1(n_2/n_1))/(\omega_1\langle R^2\rangle) = (n_2/n_1)+$ cst. These plots are shifted to the left by 1 from those of Fig. 2 and Fig. 3, as all measurements are with respect to the image attractor (with $k = 1$) in Figs. 5 and 6 instead of the original attractor ($k = 0$ in Figs. 2 and 3).

VII. REMARKS

It is useful to make a number of remarks here.

A. Autonomous vs. Nonautonomous

The autonomous-nonautonomous dichotomy is useful but not rigid. It is possible to rewrite a periodically driven system as an autonomous system. This is done for the van der Pol system (6) by introducing two new

variables, c and s (for example), that satisfy the equations $\dot{c} = -\omega_d s, \dot{s} = +\omega_d c$, and replacing the sine term in Equ. (6) by the solution s to this differential equation. In this way the nonautonomous van der Pol equation, a periodically driven system whose dynamics lie in $D^2 \times S^1$, is represented as an autonomous dynamical system in the phase space R^4. The solution exists in a three-dimensional manifold in R^4: this manifold is topologically $D^2 \times S^1$.

It has been argued that it should be possible to write certain classes of autonomous dynamical systems in nonautonomous form [4]. This class includes equations that generate strange attractors that exist within bounding tori of genus one [11, 12]. The Rössler equations are an example of such a set of equations, for normal parameter values. The basic idea is that it should be possible to find a 1-1 relation between the dynamical variable t and the geometric coordinate θ so that the equations can be written as $dx_1/d\theta = f_1(x_1, x_2, \theta), dx_2/d\theta = f_2(x_1, x_2, \theta)$. If such a transformation is possible, the standard Rössler strange attractor(s) would show no internal symmetry of the type exhibited by the standard two-dimensional nonlinear oscillators, and we would not have to spend time removing this symmetry. In this case the Rössler attractor itself would be the "universal image attractor" from which an entire two-parameter family of attractors (n_1, n_2) could be constructed. The two attractors $(2, -1)$ and $(2, +1)$ in this Rössler family are shown in Fig. 7, just to show that this really can be done. The coordinate $X(\theta)$ is the mean radius and Y is its derivative: $Y(\theta) = dX/d\theta$.

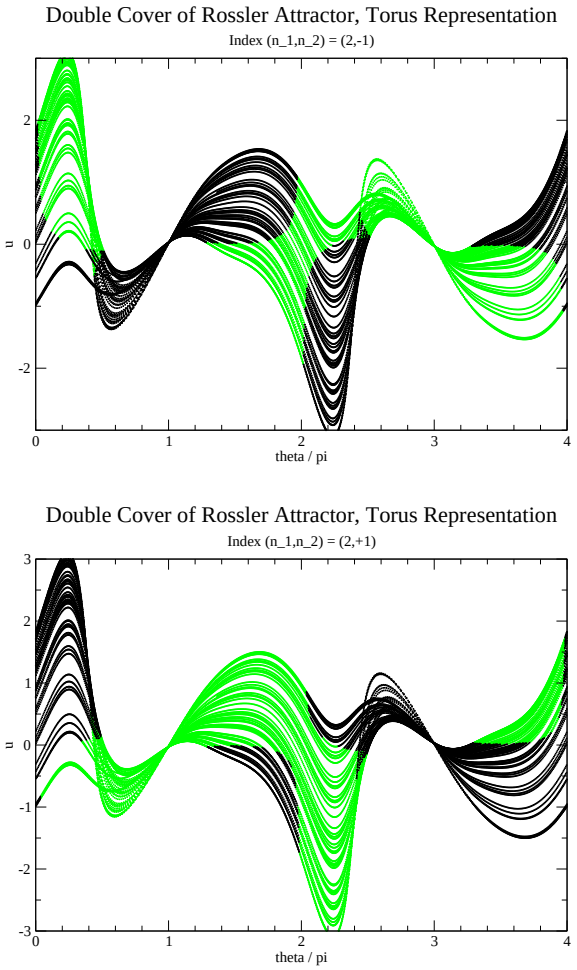

FIG. 7: Two double covers of the universal image Rössler attractor are shown. They have quantum numbers $(n_1, n_2) = (2, -1)$ (top) and $(2, +1)$ (bottom).

B. One Slight Complication

The presentation in this paper would have been more straightforward if we could have begun our discussion directly with the universal image attractor. All the most familiar examples of periodically driven dynamical systems are two dimensional nonlinear oscillators with inversion symmetry. As such, the strange attractors they generate have an internal symmetry. Sect. III was devoted to getting rid of this symmetry using a $2 \rightarrow 1$ local diffeomorphism. The general approach, introducing the pair of quantum numbers (n_1, n_2) in Sect. V, was delayed by the need to remove the internal symmetry.

If we could have begun with a description of the Rössler attractor as generated by a nonautonomous set of equations, following suggestions made elsewhere [4], this detour (Sect. III) could have been avoided.

C. Quantum Numbers

The strange attractors in this two-parameter class (n_1, n_2) of strange attractors are everywhere locally diffeomorphic with each other, and to the universal image attractor. The quantum numbers are integers related to the two generators of the homotopy group of the boundary of the torus. The quantum number n_1 describes quantization in the longitudinal direction. After n_1 intervals, each of duration T_1, the attractor satisfies periodic boundary conditions. The quantum number n_2 describes quantization in the meridional direction. When the attractor satisfies the boundary conditions in the flow direction, it has rotated through n_2 full rotations in the meridional direction.

D. Geometry, Dynamics, Topology

Tools that have been used to analyze strange attractors come from three branches of mathematics or physics: geometry, dynamics, and topology. Geometric measures include the full panoply of fractal dimensions [13]. Dynamical measures include the spectrum of Lyapunov exponents [14] and estimates of a Lyapunov dimension. Topological tools include linking numbers and relative rotation rates, used to determine their organization and the knot

holder or branched manifold that organizes all the orbits and identifies the mechanism generating chaotic behavior [10, 15–17]. Geometric and dynamical measures are diffeomorphism invariants. They are also invariant under local diffeomorphisms. As a result, all strange attractors (n_1, n_2) share an identical spectrum of fractal dimensions and Lyapunov exponents. These measures are unable to distinguish any of these strange attractors from any of the others. However, each strange attractor (n_1, n_2) has a spectrum of orbits that is uniquely determined from: (a) the spectrum of orbits in the universal image attractor; (b) the order n_1 of the cover; and (c) the global torsion n_2 of the cover. These topological fingerprints serve uniquely to distinguish cover (n_1, n_2) from $(n_1, n_2)'$.

E. Mathematical Descriptions

The construction of large classes of strange attractors presented in Sect. V has both a mathematical and a physical motivation. On both sides there is a simple description and a more complicated description. In the current subsection we present the simple and sophisticated mathematical descriptions. In the following subsection we present the simple and sophisticated physical descriptions.

Simple Mathematical Description: Imagine a strange attractor embedded inside a torus. Cut the torus at $\theta = 0$ and straighten it out so that the axis of the torus is a straight line. The intersection of the strange attractor at the section $\theta = 0$ is identical to the intersection at $\theta = 2\pi$ (periodic boundary conditions). Now rotate one end through p/q full twists. It is assumed that the rotation angle in the rest of the torus is proportional to distance between $\theta = 0$ and $\theta = 2\pi$, so for example the (surface of) section at θ rotates through angle $(p/q) \times \theta$. If p/q is not an integer, periodic boundary conditions at the two ends are no longer satisfied. Now place a copy of this twisted torus end to end with the original, matching up the $\theta = 0$ end of the copy with the $\theta = 2\pi$ end of the original. If $2 \times p/q$ is not an integer, boundary conditions are still not satisfied. Repeat this process. Eventually, q copies placed back to back in this way will satisfy periodic boundary conditions as θ increases from 0 to $2\pi \times q$. If p and q are not relatively prime, periodic boundary conditions will be achieved sooner. The strange attractor inside this torus of "length" $q \times 2\pi$ is the cover with quantum numbers $(n_1, n_2) = (p, q)$. It is clearly a q-fold cover of the original that is everywhere locally diffeomorphic with the original, that rotates p full turns before closing up.

Sophisticated Mathematical Description: At every point in the manifold S^1_θ it is possible to specify a coordinate system for D^2. One erects a frame bundle with frame group $SO(2)_\phi$, parameterized by angle ϕ (orthogonal rotations of coordinate system choice (X, Y) for any value of θ in S^1_θ) on the closed one-manifold S^1_θ. The choice of frame constitutes the identification of a section in the frame bundle. As one travels around S^1_θ from $\theta = 0$ to $\theta = 2\pi$ the coordinate frame rotates through k full turns as ϕ increases from $\phi = 0$ to $\phi = 2\pi \times k$.

If $k = p/q$ is not an integer, as θ returns to 2π the angle ϕ does not return to an integer multiple of 2π. We no longer have a section (one point in each fiber over θ) in the frame bundle. Rather, the bundle consists of q points over each point in the base manifold. Instead of a section we have a multisheeted cover of a section, similar to the two-sheeted cover of the square root function $z \to \sqrt{z}$ in complex analysis. In fact, the q-sheeted "covering section" is *exactly* like the complex covering sheet of the map $z \to (z^p)^{1/q}$. A group C_q acts on the points on any fiber through the representation $\Gamma^p(\gamma) = e^{i2\pi p/q}$, where γ is a rotation through $2\pi/q$ radians. This process amounts to parallel transport of a coordinate system along the manifold S^1_θ until it returns to its original orientation after q full circles, during which time $SO(2)_\phi$ rotates through p full rotations: $\Delta\theta = 2\pi q$ and $\Delta\phi = 2\pi p$.

F. Physical Descriptions

As stated above, we provide an analysis of our procedure based on elementary physics first. Subsequently we present a more sophisticated description.

Simple Physical Description: Assume that the coordinates (X, Y) describe the position of a particle of mass m in the plane R^2. This particle is acted on by forcing functions as given in Equ. (1b). We assume that the motion is bounded, recurrent, and nonperiodic, so that the trajectory lies on a strange attractor in the phase space $D^2 \times S^1$ ($D^2 \subset R^2$, since the motion is bounded). The average angular momentum and kinetic energy of the particle are as presented in Equs. (8) and (9) ($m = 1$). In a rotating coordinate system the equations of motion are as shown in Equ. (5). The angular momentum and kinetic energy in the rotating coordinate system are as given in Equs. (10) and (11). From this analogy it is no surprise to find a Coriolis term in the equations of motion (5), an $\Omega \cdot \mathbf{L}$ term in Equ. (11), and centrifugal terms in Equs. (10) and (11).

Sophisticated Physical Description: We have created a whole series of strange attractors from a single strange attractor almost from "thin air." We did this using two principles from classical physics and two from modern physics.

At the classical level we rely on the Principles of Relativity and Equivalence. Assume two observers, Alice and Bob, observe the dynamics. Alice sits in an inertial coordinate system and observes the development of the universal image strange attractor. Bob observes from a uniformly rotating coordinate system. The Principle of Relativity guarantees that either can describe what the other sees, algorithmically, through invertible coordinate transformations. The Principle of Equivalence guarantees that if "the rest of the universe" "looks the same" to Alice and Bob, Alice can use Bob's description to predict

the existence of a strange attractor that Bob observes, *and that attractor must exist*.

On the modern physics side, we use two properties imposed on bound-state wave functions. These are square-integrability and single valuedness. A standard condition used to define strange attractors is that the motion is *bounded*. This is analogous the the $\mathcal{L}^2$ condition on bound state wavefunctions. The other condition is single valuedness. We have imposed this to demand that the strange attractor as observed by Bob in his rotating coordinate system closes up by making p roations in q revolutions.

G. Are These All the Covers?

No. Not by a long shot.

These are all the locally diffeomorphic covers in the *intrinsic* torus $D^2 \times S^1$ [4, 5, 18, 19].

The torus itself can be embedded into R^3. There are many ways to embed a torus into R^3 [20]. The most usual one is the "natural embedding." This embedding has the center line of the torus following a circle in the plane. The centerline can be mapped onto any closed curve in R^3. These are all known, if not completely classified. Each of the strange attractors (n_1, n_2) in the intrinsic torus $D^2 \times S^1$ can be embedded into R^3 inside an *extrinsic* torus whose center line follows one of the knots that have been so thoroughly studied, for example the trefoil, granny, or square knot [5].

It is also possible to find strange attractors that are covers of the universal image in bounding tori of genus $g > 1$ [11, 12, 20]. For example, the Rössler attractor has been lifted to a double cover in a genus-three torus [5, 8]. That cover is very similar to the Lorenz attractor [21, 22]. The number of bounding tori of genus g increases exponentially with $g - 1$, with "entropy" [23]

$$\lim_{g\to\infty} \frac{\log N(g)}{g-1} \to 3 \tag{15}$$

This leaves room for a great many more topologically distinct covers that are locally identical to any universal image strange attractor than even the large number parameterized by the quantum numbers (n_1, n_2) described in this paper.

VIII. SUMMARY AND CONCLUSIONS

We have described nonautonomous dynamical systems in three dimensions. These have taken the form of periodically driven two dimensional nonlinear oscillators that possess an inversion symmetry. We have described projections to locally diffeomorphic $2 \to 1$ images using harmonic rotations, two of which are to the van der Pol planes ($k = \pm 1$). By introducing torsion and energy integrals we have been able to identify a universal image attractor uniquely.

We have introduced subharmonic rotations to lift the universal image to n_1 fold covers, with $n_1 \geq 1$. These covers are identified by two relatively prime integers, (n_1, n_2). We have called these integers quantum numbers because they arise by enforcing periodic boundary conditions. We have computed the torsion and energy integrals for many members of this class of covers numerically and for all members analytically. All strange attractors (n_1, n_2) are locally diffeomorphic and topologically distinct. They have identical spectra of fractal dimensions and Lyapunov exponents but each carries a different topological signature, consisting of its spectrum of periodic orbits and the linking numbers and relative rotation rates of these orbits. The cover $(2, -1)$ of the universal image strange attractor is the original van der Pol attractor. This has also been done for the Rössler attractor, expressed in a torus representation.

Many influences have contributed to the approach to creating new strange attractors from old described here. Some of these influences have been discussed in the Remarks Section.

Acknowledgements: The author thanks M. Lefranc, C. Letellier, and G. Naber for useful discussions and encouragement.

[1] E. A. Jackson, *Perspectives in Nonlinear Dynamics, Volumes 1 and 2*, Cambridge: University Press, 1990.
[2] E. N. Lorenz, Deterministic nonperiodic flow, *Journal of Atmospheric Science*, **20**, 130-141, 1963.
[3] O. E. Rössler, An equation for continuous chaos, *Physics Letters A*, **57** (2), 397-398, 1976.
[4] R. Gilmore and M. Lefranc, *The Topology of Chaos*, NY: Wiley-Interscience, 2002.
[5] R. Gilmore and C. Letellier, *The Symmetry of Chaos*, unpublished.
[6] R. Miranda and E. Stone, The proto Lorenz system, Phys. Lett. A, **178**, 105-113 (1993).
[7] C. Letellier and R. Gilmore, Covering dynamical systems I: Two-fold covers, Physical Review **E63**, 016206:1-10 (2001).
[8] R. Gilmore and C. Letellier, Dressed symbolic dynamics, Phys. Rev. **E67**, 036205 (2003).
[9] R. Gilmore & J. W. L. McCallum, Structure in the bifurcation diagram of the Duffing oscillator, *Physical Review E*, **51** (2), 935-956, 1995.
[10] H. G. Solari and R. Gilmore, Relative rotation rates for driven dynamical systems, Phys. Rev. A**37**, 3096-3109 (1988).
[11] T. D. Tsankov and R. Gilmore, Strange attractors are classified by bounding tori, Phys. Rev. Lett. **91**(13), 134104 (2003).
[12] T. D. Tsankov and R. Gilmore, Topological aspects of the structure of chaotic attractors in $\mathbb{R}^3$, Phys. Rev. E**69**(13),

056206 1-11 (2004).
[13] C. Grebogi, E. Ott, and J. A. Yorke, Phys. Rev. A**37**, 1711 (1988).
[14] A. Wolf, J. B. Swift, H. L. Swinney, and J. A. Vastano, Determining Lyapunov exponents from a time series, Physics D**16**, 285-317 (1985).
[15] N. B. Tufillaro, H. G. Solari & R. Gilmore, Relative rotation rates: Fingerprints for strange attractors, Physical Review A, **41**, 5717-5720, 1990.
[16] G. B. Mindlin, X.-J. Hou, H. G. Solari, R. Gilmore and N. B. Tufillaro, Classification of strange attractors by integers, Phys. Rev. Lett., **64**, 2350-2353 (1990).
[17] G. B. Mindlin, H. G. Solari, M. A. Natiello, R. Gilmore and X.-J. Hou, Topological analysis of chaotic time series data from the Belousov–Zhabotinski reaction, J. Nonlinear Sci., **1**, 147-173 (1991).
[18] D. Rolfsen, *Knots and Links*, AMS Chelsea Publishing, Providence, RI, 1990.
[19] Jeffrey R. Weeks, *The Shape of Space*, Marcel Dekker, 2002.
[20] T. D. Tsankov, A. Nishtala, and R. Gilmore, Embeddings of a strange attractor into R^3, Phys. Rev. E **69**, 056215 1-8 (2005).
[21] G. Byrne, R. Gilmore & C. Letellier, Distinguishing between folding and tearing mechanisms in strange attractors, *Physical Review E*, **70**, 056214, 2004.
[22] C. Letellier, T. D. Tsankov, G. Byrne & R. Gilmore, Large-scale structural reorganization of strange attractors, *Physical Review E* **72** (1), 026212, 2005.
[23] J. Katriel & R. Gilmore, Entropy of bounding tori, *preprint*.